Int. J. Electrochem. Sci., 14 **(2019)** 11651 – 11662, doi: 10.20964/2019.12.03

International Journal of ELECTROCHEMICAL SCIENCE
www.electrochemsci.org

Short Communication

Effect of Cathode Feed Mode on Electrochemical Machining of Diamond Hole

Yafeng He[1,2], Weiming Gan[1,2], Feihong Yin[1], Jianshe Zhao[3],Bo Xu[1],Xiaofeng Wu[1]

[1] Department of Aeronautics and Mechanics, Changzhou Institute of Technology, Changzhou, 213002, P.R.China
[2] Jiangsu Key Laboratory of Special Processing, Changzhou, 213002, P.R.China
[3] Nanjing University of Aeronautics and Astronautics, Jiangsu Key Laboratory of Precision and Micro-Manufacturing Technology, Nanjing, 210016, P.R.China
*E-mail: 460465979@qq.com

Received: 18 May 2019 / *Accepted:* 30 August 2019 / *Published:* 29 October 2019

Diamond holes are typically produced with small corner radii and high surface quality. Depending on the characteristics of the diamond structure, the influence of the tool-cathode feed mode on the diamond hole formation can be calculated by a numerical method based on analyzing the forming process of a diamond hole using electrochemical machining. The current density in the diamond-hole electrochemical machining position changes depending on whether the tool cathode does a straight-line or vibration feed. The effects of different vibration amplitudes and frequencies on the current density of a diamond-hole surface are discussed. The results show that the vibration feed of the tool cathode is beneficial for creating a uniform electric field in the diamond-hole electrochemical machining and for avoiding electric-field distortion. The three-dimensional morphology of the diamond-hole samples obtained by electrochemical machining experiments is in good agreement with the theory. It was also verified that the tool-cathode vibration feeding can improve the accuracy of the diamond-hole electrochemical machining.

Keywords: Diamond hole; electrochemical machining; current density; tool-cathode feeding mode

1. INTRODUCTION

A diamond air grille is an important part of an aircraft; it has smaller edge radii and corners and a higher surface quality. Considering the characteristics of rhombic geometry, a traditional cutting tool has poor rigidity and accessibility, an obvious thermal effect in laser processing, immature technology in three-dimensional printing, low efficiency in electrical-discharge machining (EDM) and wire EDM, and the layers easily melt and solidify. In contrast, electrochemical machining (ECM) has the advantages of a lossless tool cathode, no residual stress, good surface quality, and high processing efficiency [1]. It

can provide a low-cost and high-performance method for processing diamond holes.

In recent years, hole ECM has attracted wide attention from scholars at home and abroad. They have established multi-physical field coupling models and used finite-element or theoretical methods to calculate the coupling model, and changes in the electric field, electrolyte flow rate, H_2 bubble rate, and the electrolyte temperature in the machining gap [2]. For example, F. Klocke established that material removal in ECM is more than that in conventional EDM. A coupled physical field model has been used to study the variation of the electric field and flow field [3]. Changing the tool-cathode feeding mode accelerates the electrolyte renewal speed, promotes the timely discharge of electrolyte products, and is more conducive to achieving a uniform electrolyte distribution in the processing area; thus, stabilizing the processing process. For example, Zhao Jianshe and others used the vibration feed to improve the stability of diamond-hole ECM [4–6].

The tool-cathode structure also has a direct influence on the stability of hole ECM. Researchers have found that when the cathode rotates at a high speed, the centrifugal effect of the spiral cathode significantly enhances the electrolyte renewal and discharge capacity. In addition, the electrolyte disturbance effect accelerates the discharge of electrolyte products, thereby improving the stability of the processing [7, 8]. Mitsuo Uchiyama designed a tool-cathode structure and machined curved holes with diameters less than 6 mm by means of ultrasonic vibration[9].

In addition, to improve the ECM accuracy, cathode side-wall insulation is the most direct method of reducing secondary corrosion and the taper of the machined surface. Research indicates that the side-wall insulating layer effectively prevents electronic penetration, shields the side wall from stray electric fields, and significantly improves the processing accuracy [10]. The auxiliary anode method involves covering the thin metal layer of the tool-cathode side wall by an insulating layer. By keeping the same potential between the metal layer and the workpiece, the relative potential between the side wall and the thin metal layer is zero, this reduces the stray corrosion of the side wall and improves the forming accuracy of the parts [11, 12]. Some scholars have carried out experiments to optimize the process parameters so as to improve the accuracy of ECM[13，14].

From the above literature, we can see that many important achievements have been made in hole ECM. However, due to the interaction of various factors, the electrolysis process is complex, and its processing accuracy needs further research. Therefore, this study takes the diamond hole as the research object, analyzes the electric-field distribution in the diamond-hole ECM process, explores the relationship between the tool cathode's linear feed and vibration feed modes on the current density of a diamond hole, and carries out a diamond-hole ECM experiment. It aims to obtain the diamond-hole forming rule and improve the processing precision, which can provide a theoretical reference for the electrochemical machining of special holes.

2. EXPERIMENTAL

2.1 Principle of diamond hole ECM

During the electrochemical machining of a diamond hole, the electrolyte flows at a high speed through the tool cathode's liquid tank into the gap between the tool cathode and the workpiece. Under the electrochemical reaction, the workpiece dissolves. The ECM process can be divided into the initial

state, feed state, and equilibrium state, as shown in Figure 1. At the beginning of the machining, the tool cathode maintains a certain initial clearance with the workpiece, as shown in Figure 1 (a). As the processing progresses, the tool cathode continues to feed and the workpiece continues to dissolve, as shown in Figure 1 (b). When the feed speed of the tool cathode is equal to the dissolution speed of the workpiece, as shown in Figure 1 (c), the electrochemical machining of the diamond hole enters a balanced state until the processing is completed.

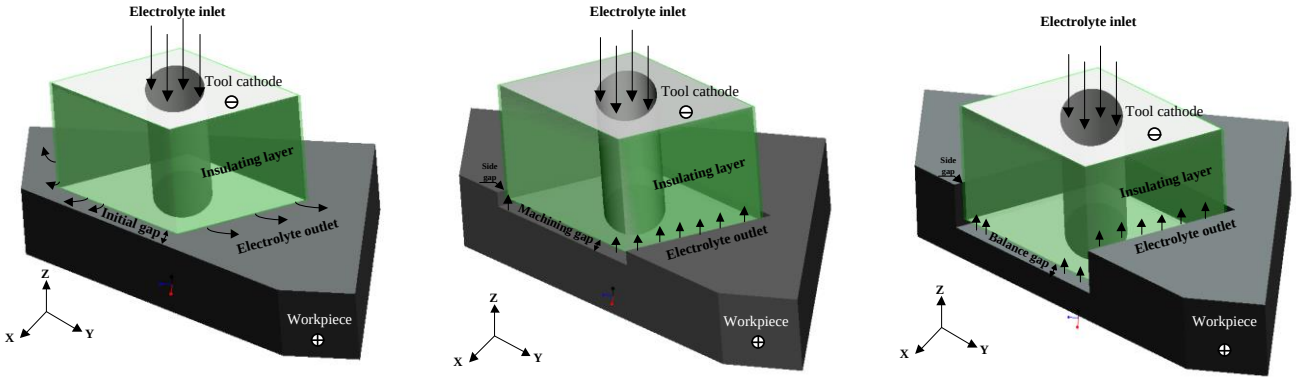

(a) Initial state (b) Feed state (c) Equilibrium state

Figure 1. Diamond-hole electrochemical machining schematic

2.2 Diamond-hole formation analysis

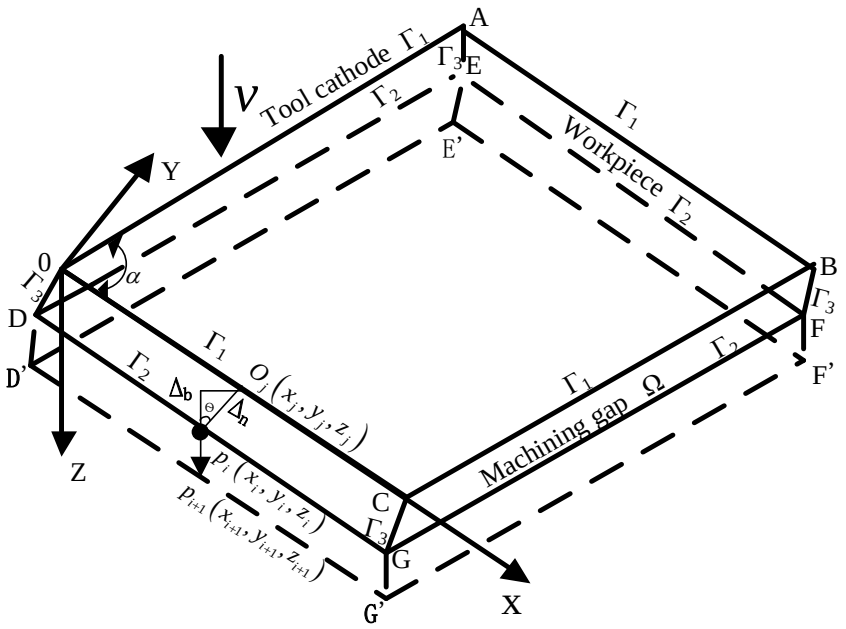

Figure 2. Forming schematic of a diamond hole by electrochemical machining

The diamond-hole forming process is shown in Figure 2. The electrolyte flows into the machining gap at a high speed. Under the action of an applied electric field, the positive ions generated in the electrolyte move towards the tool cathode and the negative ions move towards the workpiece. This forms

a current field in the machining-gap area.

The electric field model in the gap of the diamond-hole electrochemical machining is as follows:

$$\frac{\partial^2\phi}{\partial x^2}+\frac{\partial^2\phi}{\partial y^2}+\frac{\partial^2\phi}{\partial z^2}=0 \quad \text{Within the machining gap region } \Omega \qquad (1)$$

$$\begin{cases} \phi_a = U \\ \dfrac{\partial\phi}{\partial n}=\dfrac{\eta_0}{\eta}\dfrac{i_0}{k}\cos\theta \end{cases} \quad \text{On the workpiece boundary surface } \Gamma_2 \qquad (2)$$

$$\phi_c = 0 \quad \text{On the workpiece boundary surface } \Gamma_1 \qquad (3)$$

$$\frac{\partial\phi}{\partial x}=\frac{\partial\phi}{\partial y}=0 \quad \text{On the electrolyte boundary surface } \Gamma_4 \qquad (4)$$

Formulae (1)–(4): ϕ and U are the potential of each point in the electric field; n is the normal coordinate of the surface of the anode; $è$ is the angle between the cathode feed speed and the normal direction of the anode surface; $ç$ is the current efficiency; $ç_0$ is the $è$=0 current efficiency; i_0 is the $è$=0 normal current density on the anode surface; and k is the conductivity of the electrolyte.

Suppose that the workpiece surface is a closed surface composed of points DEFG in Figure 2 at time t_1. The anode surface of the workpiece is formed after Δt time while the workpiece surface dissolves continuously. For a closed surface composed of D'E'F'G', the potential of P (x, y, z) taken at any point on the workpiece surface is ϕ_p.

According to the workpiece dissolution theory in ECM, the dissolution rate of the workpiece material is as follows:

$$v_a=\eta\omega k\frac{\partial\phi}{\partial n} \qquad (5)$$

When the relative position between the workpiece and the tool cathode no longer changes, i.e., it reaches the equilibrium state, then:

$$i=-k\frac{\partial\phi}{\partial n} \qquad (6)$$

$P_i\ (x_i, y_i, z_i)$ at any point on the workpiece surface is transformed to $P_{i+1}\ (x_{i+1}, y_{i+1}, z_{i+1})$, whose transformation relationship is:

$$\begin{cases} x_{i+1}=x_i+v_{ax}\Delta t \\ y_{i+1}=y_i+v_{ay}\Delta t \\ z_{i+1}=z_i+v_{az}\Delta t-v\Delta t \end{cases} . \qquad (7)$$

It can be seen from formula (7) that the change of the electrochemical machining of diamond holes is mainly related to the distribution of the potential.

According to the variation principle, the potential distribution of the machining gap is as follows:

$$I(\phi)=\frac{1}{2}\iiint_{\Omega}\left[\left(\frac{\partial\phi}{\partial x}\right)^2+\left(\frac{\partial\phi}{\partial y}\right)^2+\left(\frac{\partial\phi}{\partial z}\right)^2\right]dxdydz-\iint_S\frac{\eta_0 i_0}{\eta k}\phi\cos\theta ds \qquad (8)$$

Considering the boundary conditions and using the shape-function method, the total stiffness matrix is:

$$\begin{bmatrix} K_{11} & K_{12} & 0 & 0 & 0 & 0 \\ K_{21} & K_{22} & K_{23} & 0 & 0 & 0 \\ 0 & K_{32} & K_{33} & K_{34} & 0 & 0 \\ 0 & 0 & K_{43} & K_{44} & K_{45} & 0 \\ 0 & 0 & 0 & K_{54} & K_{55} & K_{56} \\ 0 & 0 & 0 & 0 & K_{65} & K_{66} \end{bmatrix} \begin{bmatrix} \phi_1 \\ \phi_2 \\ \phi_3 \\ \phi_4 \\ \phi_5 \\ \phi_6 \end{bmatrix} = \begin{bmatrix} c_1 \\ 0 \\ 0 \\ 0 \\ 0 \\ 0 \end{bmatrix} \quad (9)$$

Among them, c_1 is the coordinate value of the workpiece anode boundary, ϕ_1 is the potential of the workpiece anode surface, and ϕ_6 is the potential of the tool-cathode surface.

$$\begin{cases} \phi_2 = -K_{12}^{-1}\left(K_{11}\phi_1 - c_1\right) \\ \phi_3 = -K_{23}^{-1}\left(K_{21}\phi_1 + K_{22}\phi_2\right) \\ \phi_4 = -K_{34}^{-1}\left(K_{32}\phi_2 + K_{33}\phi_3\right) \\ \phi_5 = -K_{45}^{-1}\left(K_{43}\phi_3 + K_{44}\phi_4\right) \\ \phi_6 = -K_{56}^{-1}\left(K_{54}\phi_4 + K_{55}\phi_5\right) \end{cases} \quad (10)$$

By analogy, the expression of the potential distribution in the ECM gap area can be obtained as follows:

$$\phi_{i+1} = -K_{i,i+1}^{-1}\left(K_{i,i-1}\phi_{i-1} + K_{ii}\phi_i\right). \quad (11)$$

2.3 Numerical calculation of diamond hole electrochemical machining

2.3.1 Analytical model of the diamond-hole electrochemical machining

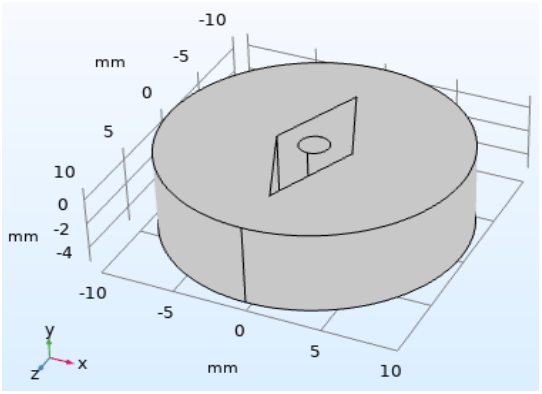

Figure 3. Analytical model of the electrochemical machining of a diamond hole

The electrochemical machining of a diamond hole depends on the continuous feed of the cathode rod and the anodic dissolution of the workpiece. The processing model mainly consists of the cathode rod, workpiece, and electrolyte cavity, To calculate the formation change of the diamond hole, a calculation model of the processing area is established, as shown in Figure 3. a closed area is composed of the workpiece, cathode, and electrolyte.

2.3.2 Calculation method and parameters of diamond hole ECM

The electrochemical machining of a diamond hole is a dynamic process over time, and an electric field is the main factor affecting the forming process. In the numerical calculation of a diamond hole,

the arbitrary Lagrangian-Eulerian (ALE) moving-mesh algorithm is used to establish the relationship between the workpiece-dissolution field and the electric field, to realize a change in the machining contour position.

The calculation parameters are as follows:

Parameter	Unit	Range
Processing voltage	V	18
Power-supply frequency	Hz	1000
Cathode linear-feed speed	mm/min	0.35
Processing time	min	7.0
Conductivity	S/mm	0.012
$NaNO_3$ electrolyte	%	10

2.3.3 Numerical calculation results of diamond tool cathode linear feed

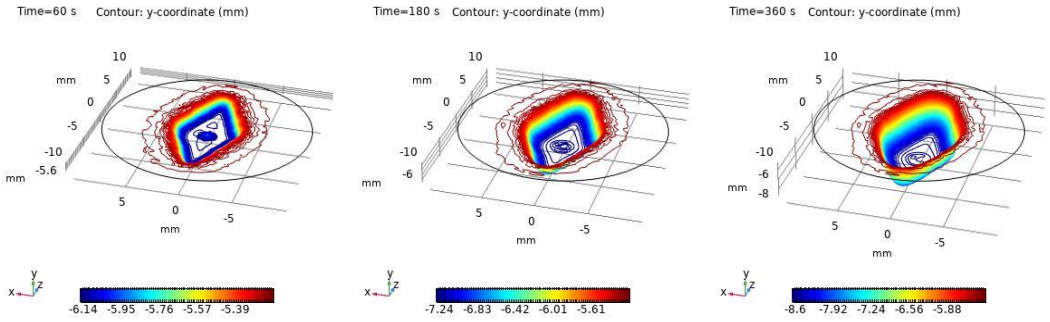

(a) t = 60 s (b) t = 180 s (c) t = 360 s

Figure 4. Diamond-hole forming profile with different processing times

Vyom Sharma has been adopted a thin copper wire of diameter 30 mm as a tool.precise micro slits to generate precise micro slits on a flat stainless steel 304 workpiece, the process was modelled in two dimensions with weak field formulation using finite element method (FEM) and the algorithm was implemented using a code in MATLAB. prediction of anode profile was done and this predicted profile was compared with the experimentally obtained profile[15]. Similarly, the finite element method is also used in this paper. the contour changes of the diamond hole at 60 s, 180 s, and 360 s are calculated using the moving-mesh algorithm. As shown in Figure 4, the clearance and corner position of the diamond hole become larger with the continuous linear feed of the tool cathode; this is due to the secondary corrosion of a stray electric field on the side wall, resulting in reduced contour-forming accuracy.

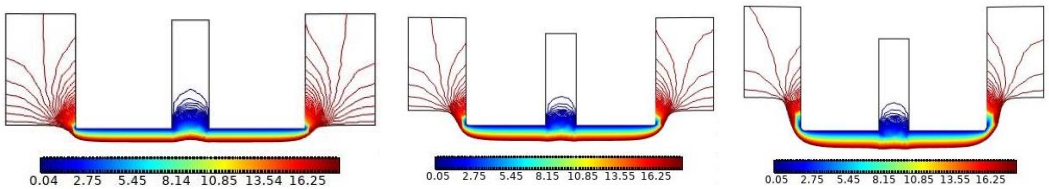

(a) t = 60 s (b) t = 180 s (c) t = 360 s

Figure 5. Potential distribution of the diamond hole profile at different processing times

As shown in Figure 5, the potential distribution along the diagonal section of the diamond hole is the same when the processing time is 60 s, 180 s, and 360 s. The potential decreases from the diamond-processing surface to the tool cathode in turn, and the electric field is concentrated at the diamond corner position, which easily rounds at the corner position.

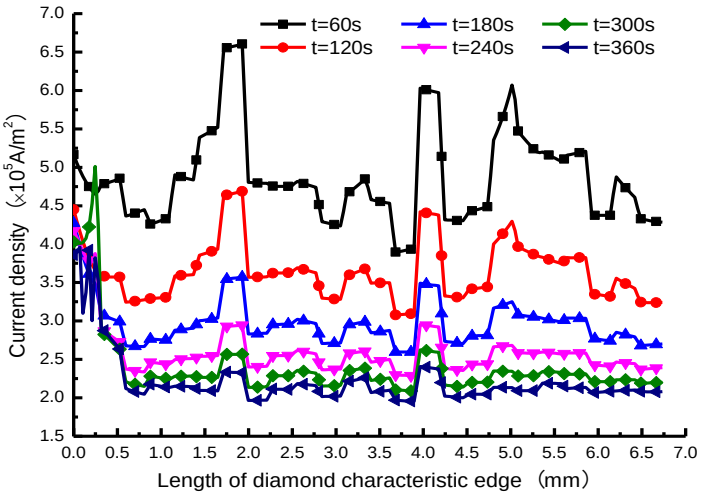

Figure 6. Current density variation of a diamond characteristic edge

The current density is the main measure of material dissolution. Figure 6 shows the variation of the current density obtained by extracting the diamond characteristic edge. The current-density distribution trend of the diamond characteristic edge is basically the same at different times, while the sudden change of the current density is obvious at the same time. This also shows that the material dissolution speed in the diamond processing area is obviously different when the tool cathode is feeding in a straight line, resulting in an uneven surface for the diamond processing.

2.4 Experimental system for diamond-hole ECM

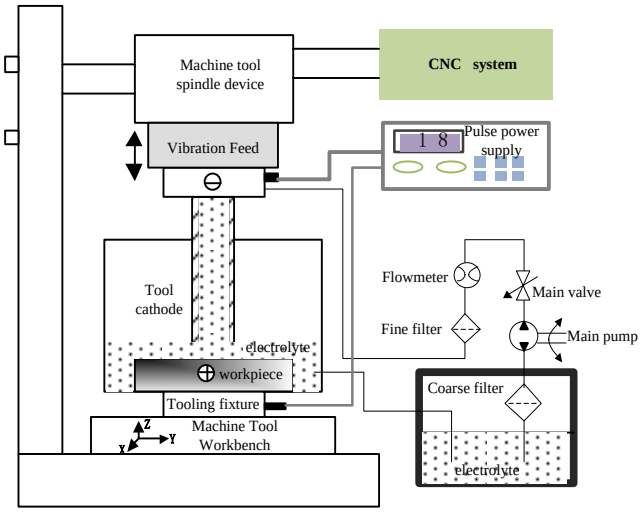

Figure 7. Electrochemical machining experiment system for diamond holes

The experimental system for diamond hole ECM, as shown in Figure 7, is mainly composed of the ECM machine tool, control system, electrolyte filtration system, and tooling fixture. The machine-tool worktable can realize X-axis and Y-axis movement. The vibration feed device is installed on the machine-tool spindle. The tool cathode is connected to the vibration device. The tool cathode can move straight, or reciprocate along the Z-axis. The workpiece is fixed on the fixture. Under the action of the main pump, the electrolyte flows at high speed into the processing area from the tool cathode through the liquid tank and through the coarse and fine filters. Under the electrochemistry action, the workpiece dissolves continuously to form diamond-shaped hole.

3. RESULTS AND DISCUSSION

3.1 Electric-field distribution on the diamond machining surface

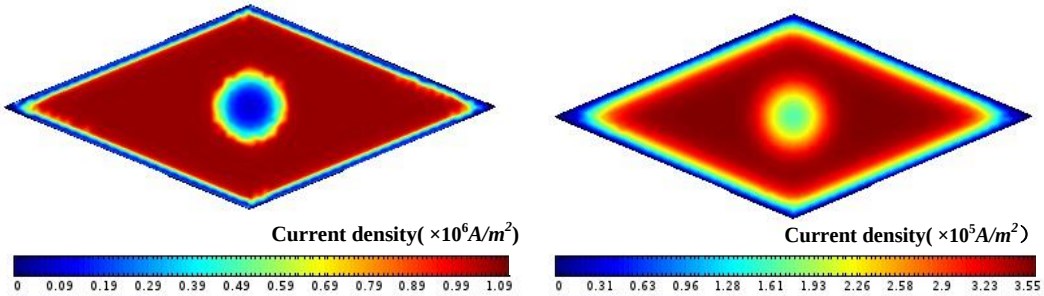

(a) Linear feed (b) Vibration feed

Figure 8. Electric-field distribution of different tool-cathode feeding modes

The electric-field distribution on the diamond working surface under different tool-cathode feeding modes is shown in Figure 8. The current density distribution on the diamond working surface is more uniform than that on the straight-line feeding. The uniformity of the electric field is improved by the tool cathode vibration. This is because the vibration of tool cathode homogenizes the electric field distribution and makes it more uniform.

3.2 Tool-cathode vibration feed for electrochemical machining

3.2.1 Current-density change of the diamond characteristic edge

The current density change of the diamond characteristic edge in a cycle is extracted. As shown in Figure 9, the change trend of the current density of the diamond characteristic edge is gentler than that of the straight-line feed, and there is no sudden change in the current density. The current density fluctuates regularly in one cycle, which is beneficial for a uniform electric field in the diamond-hole processing. This is because the tool-cathode vibration improves the stability of the flow field in the processing area. The flow-field stability maintains the conductivity without change, which makes the processing electric field more uniform.

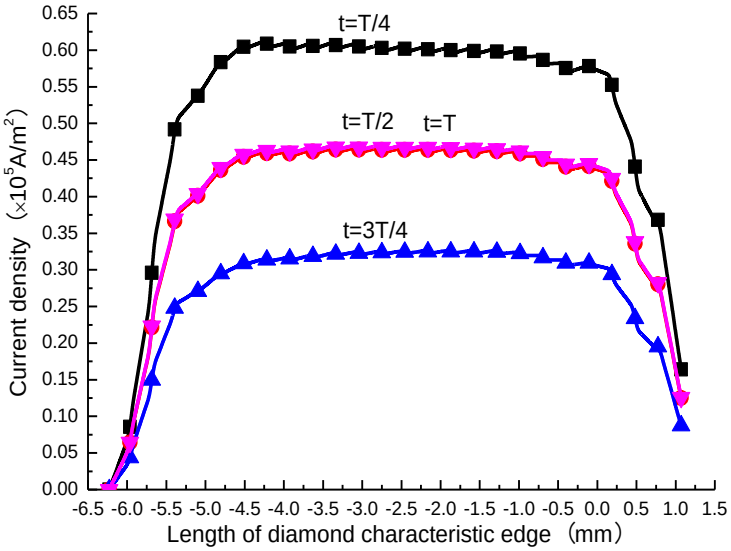

Figure 9. Current density variations in the diamond characteristic edge period

3.2.2 Effect of the vibration amplitude on the current density

A method of WEMM assisted with coupling axial and intermittent feed-direction vibrations is proposed by Haidong He,the mechanism of the mass transport in the machining gap using this method was theoretically analyzed with the results indicating that the proposed method was very beneficial for improving the mass transport rate in the machining gap, owing to the high flow velocity in both the feeding and axial directions. the intermittent feed-direction vibration increase the machining efficiency and quality [16].

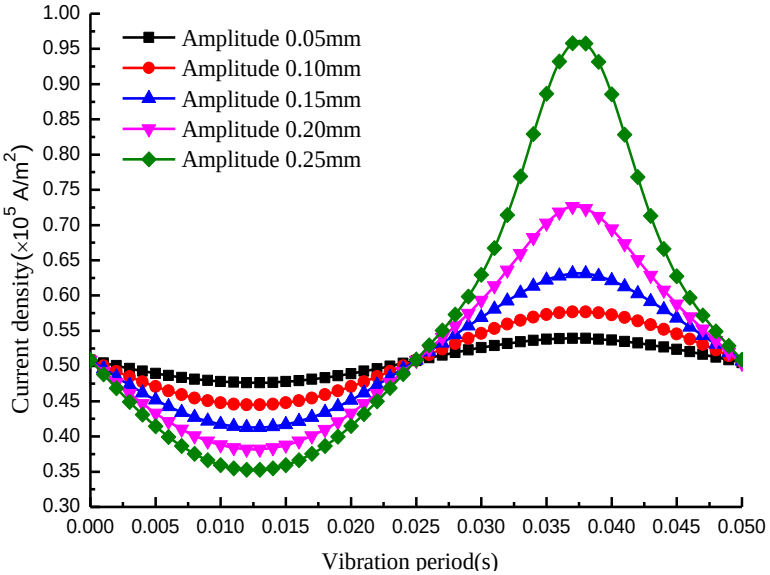

Figure 10. Relations between vibration amplitude and current density

When other conditions remain unchanged, the current density obtained by changing the vibration

amplitude changes. As shown in Figure 10, the current density obtained by the diamond-shaped processing position changes regularly and smoothly in the same vibration period under different amplitudes. As the vibration amplitude increases, the variation of the current density is also obvious. This is because the amplitude and the gap fluctuation increase. When the tool cathode is far from the sampling point, the gap is the largest and the current density is the smallest. When the tool cathode approaches the sampling point, the clearance is the smallest and the current density is the largest. with the increase of current density, the processing efficiency increases correspondingly.

3.2.3 Effect of the vibration frequency on the current density

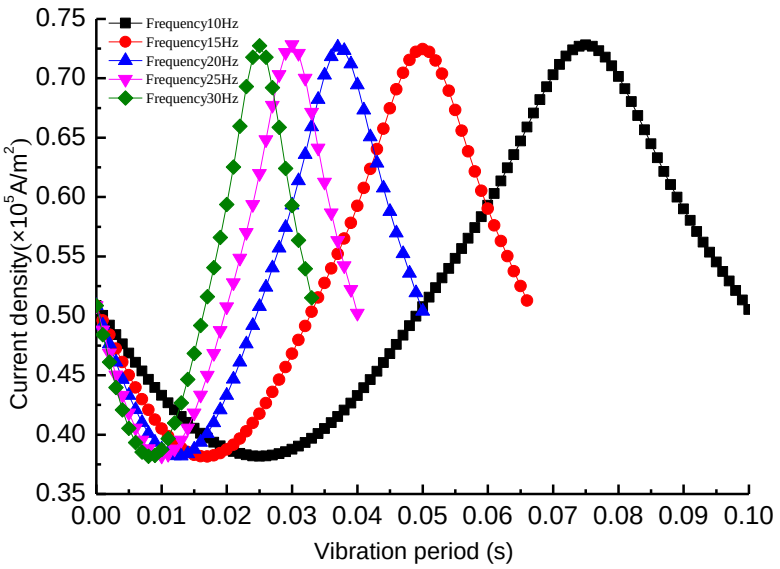

Figure 11. Relations between the vibration frequency and current density

When other conditions remain unchanged, the current-density change obtained by changing the vibration frequency is shown in Figure 11. When the vibration frequency increases, the change trend of the current density at the diamond-processing position is the same, showing a regular fluctuation. Changing the vibration frequency is helpful to improve the continuous dissolution of workpiece materials.

3.3 Three-dimensional morphology of ECM diamond-hole samples

Application of low frequency vibration to the tool electrode in electrochemical machining is one of the effective techniques for improving accuracy and quality of the machined surface[17, 18].The effect of input parameters and machining conditions on the effectiveness of tool vibration during ECM has been fully investigated. The analytical model reveals that there could be a great complexity in the relationship between the tool amplitude and the equilibrium gap size, which could lead to tool damage, if the problem has not been carefully considered[19].The processed stainless-steel diamond hole samples are shown in Figure 12. It can be seen that when the tool cathode uses a linear feed, the side wall and

corner position of the diamond hole have poor forming accuracy. When the tool cathode is fed in vibration mode, the forming accuracy of the side wall and corner is significantly improved, which is consistent with the theoretical analysis that the vibration feed can homogenize the electric field and avoid an electric-field distortion.

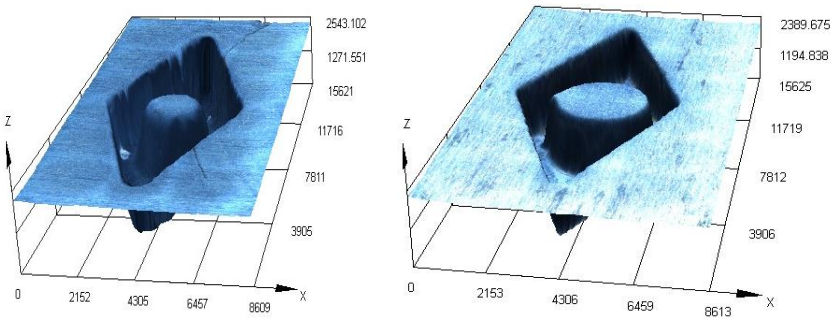

(a) Linear-feed processing specimen (b) Vibration-feed processing specimen

Figure 12. Three-dimensional morphology of samples processed by different tool-cathode feeding modes

The processing conditions are as follows:

Parameter	Unit	Range
Processing voltage	V	18
Power-supply frequency	Hz	1000
Cathode linear-feed speed	mm/min	0.35
Vibration frequency	Hz	20
Vibration amplitude	mm	0.2
Processing time	min	7.0
Inlet electrolyte pressure	MPa	0.5
$NaNO_3$ electrolyte	%	10

5. CONCLUSIONS

(1) The position radius of a diamond hole is small and the surface quality is high. Compared with other processing methods, ECM provided a low-cost and high-efficiency processing method for diamond holes.

(2) According to the analysis of the diamond-hole electrochemical forming process, the electric field model in the machining gap of the diamond hole was obtained, and the expression of the potential distribution in the processing area was established using the variation principle.

(3) Using the moving-grid algorithm, the diamond profile-change process and the potential distribution at different processing times were calculated numerically through the transformation relationship between the workpiece dissolution field and the electric field. When the tool cathode used a linear feed, the diamond corner-position roundness increased.

(4) The numerical results of the different tool-cathode feeding modes showed that when the tool-cathode feed was linear, the electric field in the diamond-shaped processing area changed dramatically; when the tool cathode vibrated in feeding, the electric field did not distort, but changed smoothly and regularly in the diamond-shaped processing position at different vibration amplitudes and frequencies. This decreased the difference in the material-dissolution rate in the processing area and improved the processing accuracy.

(5) The morphology of the samples obtained by the electrochemical machining of the diamond holes showed that the forming accuracy of the side wall and the corner position of diamond holes significantly improved when the tool cathode was fed by vibration. This also shows that the tool-cathode vibration feeding can homogenize the electric-field distribution, which is consistent with the theoretical analysis. The results also provided a theoretical basis and reference for the electrochemical machining of other abnormal holes.

ACKNOWLEDGMENTS
This work was supported by the Natural Science Foundation of JiangSu Province (BK20161193), The Natural Science Foundation of the Jiangsu Higher Education Institutions of China(19KJA430005),Key R&D Projects of JiangSu Province (BE2018067), and Jiangsu Key Laboratory of Precision and Micro-Manufacturing Technology.

References

1. M. Hackert-Oschätzchen, R. Paul, A. Martin, G. Meichsne, N. Lehnert, A. Schubert, *J. Mater. Process. Technol.,* 223 (2015) 240.
2. X. L. Fang, N. S. Qu, Y. D. Zhang, *J. Mater. Process. Technol.,* 214(2014) 556.
3. F. Klocke, M. Zeis, S. Harst, *Procedia CIRP*, 8(2013) 265.
4. J. S. Zhao, X. L. Zhang, Z. W. Yang, Y. M. Lü, Y. F. He, *Int J. Adv. Manuf. Tech.,* 91(2017)147.
5. J. S. Zhao, F. Wang, X. L. Zhang, Z. W. Yang, Y. M. Lü, Y. F. He, *Procedia CIRP*, 68(2018) 684.
6. J. S. Zhao, F. Wang, Z. Liu, X. L. Zhang, W. M. Gan, Z. J. Tian, *Chin. J. Aeronaut*, 29(2016)1830.
7. T. Paczkowski, J. Zdrojewski, *J. Mater. Process. Technol.,* 244(2017)204.
8. N. M. Minazetdinov, *J. Appl. Math. Mec*, 81 (2017)29.
9. M. Uchiyama, T. Hasegawa, *Procedia CIRP,* 68(2018) 694.
10. J. Wang, W. Chen, F. Gao, F. Z. Han, *Int J. Adv. Manuf. Tech.,* 75(2014)21.
11. N. S. Qu, X. L. Chen, H. S. Li, *Chin. J. Aeronaut*, 27(2014)1030.
12. D. Y. Wang, Z. W. Zhu, D. Zhu, *J. Mater. Process. Technol.,* 239(2017)66.
13. H. Demirtas, O. Yilmaz, B. Kanber, *J. Manuf. Process.,* 43(2019)244.
14. P. Choungthong, B. Wilaisahwat, V. Tangwarodomnukun, *Procedia Manuf.,* 30(2019)552.
15. V. Sharma, I. Srivastava, V. K. Jain, J. Ramkumar, *Electrochim. Acta,* 312 (2019) 329.
16. H. D. He, X. Zhang, N. S. Qu, Y. B. Zeng, B. W. Zhong, *J. Electrochem. Soc*,166 (2019)165**.**
17. S. H. Wang, D. Zhu, Y. B. Zeng, Y. Li, *Int J. Adv. Manuf. Tech.,* 53(2011)535.
18. B. Ghoshala, B. Bhattacharyya, *Precis. Eng,* 42(2015)231.
19. M. S. Hewidy, J. Ebeid, T. A. El-Taweel, A. H. Youssef, *J. Mater. Process. Technol.,* 189(2007) 466**.**